Studying the Effects of SiO_2 Specifications and Properties of (SiO_2/$MgCl_2$/TEOS/$TiCl_4$/$AlEt_3$) Catalyst System on Kinetic Behavior and Hydrogen Responsibility of Ethylene Slurry Polymerization

Mohammad Vakili,[1,2] Hassan Arabi,[1] Hamid Salehi Mobarakeh,[1] Mehdi Ghafelebashi[2]

[1]*Department of Polymerization Engineering, Iran Polymer and Petrochemical Institute, Tehran, Iran*
[2]*Natural Petrochemical Company Research and Technology (NPC-RT), P.O.Box:1435884711, Tehran, Iran*

Received 14 January 2010; accepted 11 April 2010
DOI 10.1002/app.32609
Published online 11 June 2010 in Wiley InterScience (www.interscience.wiley.com).

ABSTRACT: A series of silica gels with different physico-chemical properties such as average pore size diameter, pore volume, attrition quality index, and bulk density were prepared, characterized, and subjected to treatment in special thermal program. Catalyst precursors were prepared by reaction of these silica gels with dibutyl magnesium ($MgBu_2$) at 50°C and then addition of tetraethoxy ortho silicate and subsequent impregnation with titanium tetrachloride ($TiCl_4$). Polymerization of ethylene by these catalysts at comparable conditions and also at different P_{H2}/P_{C2} ratio was carried out; the results showed that support properties have significant influence on polymerization behaviors such as activity profile, productivity, and hydrogen responsibility. To quantitative analysis of the results, a new kinetic relation for rate-time profiles was derived, and these kinetic parameters were used to study and calculate of the effects of support specification. It was observed that trends of activity profiles were mainly affected by support properties and as well as P_{H2}/P_{C2} ratio. Interestingly enough, catalysts with different pore volume diameter show different behavior with variation of P_{H2}/P_{C2} ratio. Increasing in pore size diameter from 60 to 200 Å give raises catalyst activity by two times. Finally, mentioned variables were attributed to different particle growth and mechanism of fragmentation during polymerization. © 2010 Wiley Periodicals, Inc. J Appl Polym Sci 118: 2216–2224, 2010

Key words: Ziegler-Natta polymerization; polyolefin; support; kinetics; catalyst

INTRODUCTION

Silica gel in combination with alkyl magnesium is used as a support for preparation of catalysts which have beneficial morphology and improved H_2 responsibility required in gas phase preparation of polyethylene with improved optical and mechanical properties.[1–4] Most behaviors of a polymerization catalyst, e.g., fragmentation phenomena, activity profile shape, particle growth, and final polymer morphology and furthermore some properties are closely affected by support specification.[5] To explore the mechanism of particle growth and fragmentation, several methods and techniques have been applied for investigation of early stages of polymerization behavior and finding its relation to support structure parameters.[6–14] McDaniel[15,16] reported that porosity in Cr/Silica catalysts plays a major role in determining the molecular weight (MW) and molecular weight distribution, whereas pore diameter determines the fragility of catalysts, which govern the degree of fragmentation and the fragment size. With increasing porosity, the rate of polymerization increased, while pore diameter controls how easily the polymer can escape from the interior of the fragment. Also, he concluded that fragmentation is required for activity but is not the rate controlling step. Fink et al.[17,18] studied the fragmentation of metallocene catalyst supported on silica gel in propylene polymerization and correlated all discriminatory steps of rate-time profile to different step of catalyst fragmentations. Abboud et al.[13,19] studied the fragmentation of emulsion-based Ziegler-Natta catalysts and reported that catalyst based on $MgCl_2$ show a more particular fragmentation pattern and form narrow particle fragments. Polymer growth appeared to exist throughout the emulsion-based catalyst particle just from the initiation of the polymerization although the surface area and porosity were very low. Here, at the initial stages of polymerization, catalyst particles broke up and catalyst fragments emerged on the surface as plates between which the polymer was growing.[20]

For polymer growth and fragmentation of catalyst, depending upon above and others evidences, three

Correspondence to: H. Arabi (H. Arabi@ippi.ac.ir).

models have been proposed. Multigrain model that result in immediate fragmentation of the catalyst particle,[21] is one of the most popular and simple model for the particle growth in olefin polymerization.[22] According to this model, immediately when the polymerization starts, the catalyst particles break up into small fragments. In the core–shell model, also known as the layer-by-layer model, the catalyst particle does not break up at the beginning of the polymerization process. The third model is the polymeric flow model. According to this model, it is also assumed that the catalyst particles break up at the beginning of the polymerization, but polymer and catalyst fragments are taken into consideration as one phase.[23] The multigrain and polymeric flow models are the most commonly used models to explain the replication phenomena.[24]

Also various models for particle fragmentation have been presented in the literature.[25,26] One fragmentation model is a continuous bisection fragmentation model, where the catalyst support successively fragments into finer and finer fragments. In the case of shrinking core model, fragmentation proceeds from the surface to the center of the particle. According to the studies of Hammawa and Wanke,[27] the fragmentation mechanism of less fragile catalysts is the shrinking core, whereas highly friable catalysts follow the continuous bisection fragmentation model. Time profile activity of this catalyst as an important feature is related to fragmentation of porous supports as reported by Knoke et al.[28] Although better understanding of these behaviors would offer significant support to catalyst design and development, very little has been done to investigate and constructing the relation between support-catalyst-polymerization behavior and polymer properties.[29,30] The ability of the support to fragment is an essential requirement for an applicable catalyst system as fragmentation down to the nanometer scale guarantees a high activity and productivity. So, a series of specific supports and corresponding catalysts were prepared and polymerization behaviors are studied with the aim of finding out quantitative relation between catalyst/support- polymerization behavior and polymer properties.

EXPERIMENTAL

Materials

Ethylene, hydrogen, and nitrogen gases (99.99%) were, respectively, supplied by Messer Co. (Krefeld, Germany) and Roham Gas Co., (Tehran, Iran), respectively. All gases were further purified with filled columns of molecular sieves that adsorb humidity, CO_2, and sulfur compounds. Silica gels (grades 644, 633), dibutylmagnesium, tetraethoxy ortho silicate, and $SiCl_4$ were purchased from Alderich. $TiCl_4$ from Merck, triethylaluminum from Akzo Corp).

Support preparation

Some silica gels were prepared by developing methods described elsewhere.[31] In typical silica gel preparation, about 200 g of $(SiO_2)\times(Na_2O)y$ (31 wt %) solution in water was poured into a 1 L glass reactor equipped with the stirrer and temperature control, then it was diluted by additional 200 g of deionized water and cool down to below 0°C. It was titrated by H_2SO_4 (10 wt %) till pH keep hold of 5–6. The temperature of silica gel prepared was increased to 90–100°C, and it was allowed to age for different times. After aging, it was conducted to washing by enough deionized water so that the residual Na^+ content reached below 5 ppm. To reduce surface tension and in turn shrinkage effect, before drying, the water content of silica gel was replaced by a reagent with lower surface tension like acetone.

Silica gels treatments

Treatment of silica supports at elevated temperatures (200°C) drives off any moisture and rising to higher temperatures (up to 600°C) brings two neighboring hydroxyl groups to form a siloxane bridge [—Si—O—Si—] by eliminating of one molecule of water which adjust the surface [OH] groups. Here, about 10 g of silica gel was poured into the quartz glass tube within the heating zone. A preset program stated to begin dehydration, using a Eurotherm programmable temperature controller. A ramp and soak profile are shown in Figure 1.

Catalyst preparation

All catalysts were prepared as follows:

About 5 g of thermal-treated silica gel was added to 200 cc glass reactor containing 70 cc heptane. The slurry was mixed and heated to 50°C. While stirring in 200 rpm, dibutyl magnesium was added at a ratio of 1.5 mmol Mg/g silica during 1 h and was allowed to complete reaction for further 1 h. TEOS of 2.2 mmol was then added and stirred for 2 h, after that about 10 mmol of $SiCl_4$ was added and stirred for 1 h, and finally 5 mmol $TiCl_4$ was added and mixed for 1 h. The catalyst precursor was washed two times with pured hexane and dried at mild condition under N_2 purging.

Polymerization

All reagents were kept and operations carried out under N_2 blanketing. Polymerization reactions were

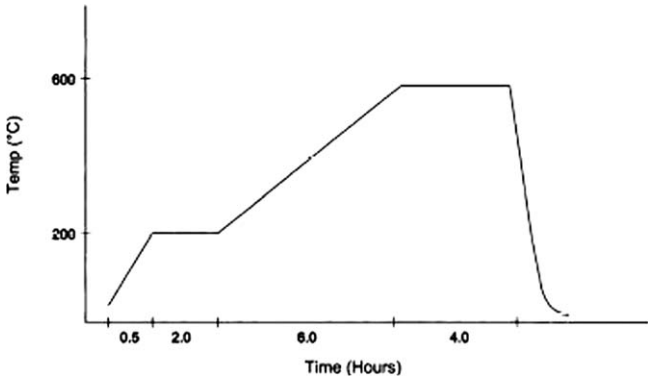

Figure 1 Typical calcination program for SiO_2 thermal treatment.[32]

carried out in a 1 dm^3 buchi reactor. In a typical experiment, *n*-hexane (solvent) and H_2 (transfer agent) were added to the reactor and after adjusting the temperature, The cocatalyst and catalyst were fed into the reactor by means of vessel connected to reactor lid. Then, the reactor was pressurized by ethylene and total pressure was maintained by ethylene feed (rate profile) during polymerization. Table II shows the polymerization conditions for different catalysts.

Characterization

Surface area, pore volume, and pore size diameters were determined by N_2-BET and BJH analyzer methods. XRD was used to determine the crystal structure of SiO_2, the instrument that used for the powder X-ray diffraction measurements was a Bruker AXS. The hydroxyl content of silicas dehydrated was characterized by titration with TiCl4 in a hexane solution. After washing and drying of titrated silica, the titanium content of the treated silica (a measure of the presence of hydroxyl groups in the silica) was determined by spectrophotometric method. The elemental analysis of laboratory prepared precursors was determined by X-Ray fluorescence spectroscopy (XRF) and Vario EL CHNOS elemental analyzer. Infrared spectra were obtained using the diffuse reflectance sampling technique. A Nicolet 7199 FT-IR spectrometer purged with dry air and equipped with a narrow band mercury-cadmium-telluride detector was used. Samples for analysis were prepared in an inert atmosphere dry box by making a 10% (w/w) dispersion of the sample in predried, ground KCl. The melt flow index (MFI) and melt flow ratio (MFR) of the produced polymer were determined by modular melt flow 7026 CEAST according to ASTM D 1238.

The frangibility of the support agglomerates is characterized by the attrition quality index (AQI) as defined by the following eq. (1):

$$(\mathrm{AQI}) = Z - Y \tag{1}$$

Z is the percentage of particles below 32 micron in the starting samples and Y is the percentage of particles below 32 micron after milling.

For measuring AQI, 2 g of SiO_2 dried at 200°C and was analyzed by sieve to determine the Z, after that, samples were milled at 450 rpm with 2 balls in Retch miller for 5 min and reanalyzed to calculate Y and AQI. All characteristic results are presented in Table I.

RESULTS AND DISCUSSION

Silica gels with different average pore size diameter from 60 to 300 Å according to methods earlier described[31] were prepared and characterized (Table I) by different techniques. And no any distinguishable peaks were observed, because of noncrystalline structure of silica gels as demonstrated in Figure 2.

TABLE I
The Characteristics of Different Supports and Related Catalysts

Catalyst	PS[a] (μm)	APD[b] (g/cm^3)	APV[c] (Å)	SA[g] (m^2/g)	(AQI%)[e]	[OH] (mmol/gr$_{Si}$)	Catalyst elemental analysis%					
							Si	Mg	Cl	Ti	C	H
*S*3(643)	35–70	1.15	150	300	10.2	0.63	42	1.4	4.3	3.7	3	0.8
S 4(633)	35–75	0.75	60	480	10.2	0.65	43	0.9	5.1	3.3	3.1	1
S 5(ES70W)	42	1.62	235 (330)[d]	276	13.1	0.58	40	1.4	5.2	5.1	4.3	1.1
S 6(Syn)[f]	32–64	1.4	184 (360)[d]	307	45	0.59	39	1.6	4.1	4.1	4	1.2
S 7(Syn)	32–64	1.5	210	286	21	0.60	41	1.7	4.6	4.9	4.6	0.8
S 8(Syn)	32–64	1.3	184	281	15	0.62	42	1.3	4.5	4.3	4	0.9

[a] Particle Size, Sieve analysis (micron).
[b] Average Pore Diameter, BJH method.
[c] Average Pore Volume, BET method.
[d] Mercury porosimetery.
[e] AQI: Attrition Quality Index.
[f] Synthesis.
[g] Specific Surface Area, BET method.

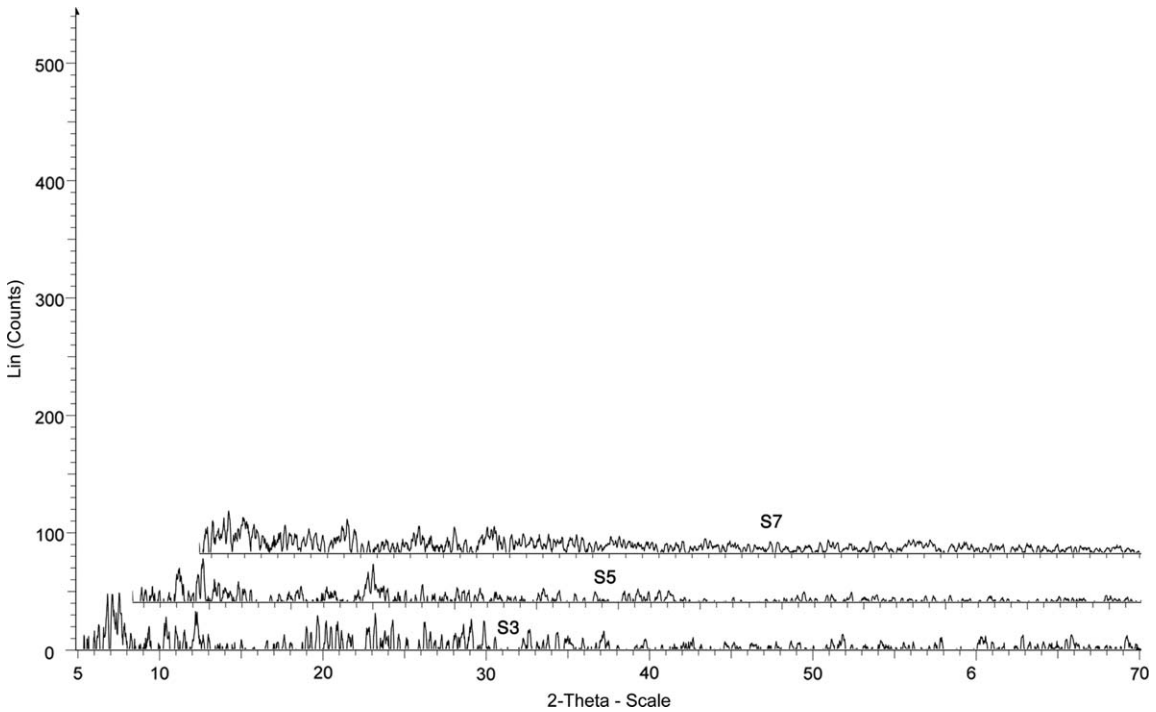

Figure 2 XRD spectrums of silica gels correspond to S3, S5, and S7 respectively.

Catalyst preparation was carried out by reaction of these silica gels with MgR_2 at 50°C and addition of TEOS as a modifier/donor and subsequent impregnation with $TiCl_4$. Figure 3 indicates FTIR spectrums of final catalyst and all intermediate materials. As it was shown, the peaks at 470 and 810 cm^{-1} are ascribed to the Si—O—Si bending vibration, that at 1100 cm^{-1} to the Si—O stretching vibration and that at 960 cm^{-1} to the Si—OH stretching vibration and a peaks at about 3400–3450 cm^{-1} are ascribed to hydroxyl groups on the surface of the silica, isolated hydroxyl groups in calcinated Silica (adsorption peak at 3400 cm^{-1} in spectrum 1) after reaction with dibutyl magnesium disappear and new peaks in 2900 cm^{-1} as an indicative of C—H bonds have been emerged. It was suggested that dibutyl magnesium reacts with isolated and siloxane bridges in calcined silica causing a ring-opening reaction of siloxane bridge giving Si—O—MgBu group and a Si—Bu group, when chlorinated with $SiCl_4$, $MgCl_2$ is formed and Si—OH group is restored (appearing peaks of 3400 cm^{-1}) and finally by reacting with $TiCl_4$ give more intensive peaks of 3400 cm^{-1} and 1640 cm^{-1}.[9]

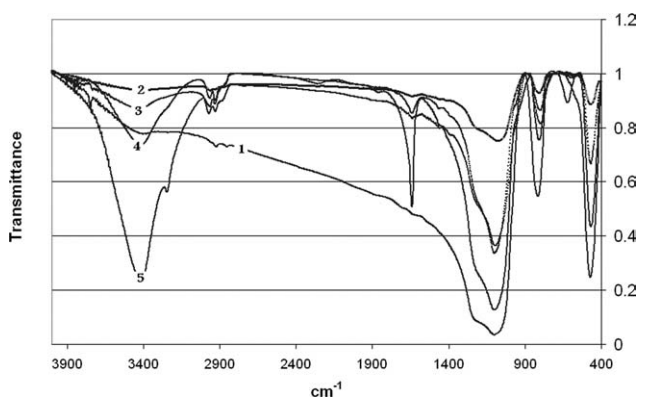

Figure 3 FTIR Spectrums of 1 calcinated silica, 2 after reaction with $Mg(Bu)_2$, 3 TEOS, 4 $SiCl_4$, and finally, 5 $TiCl_4$, respectively.

Polymerization of ethylene in the same conditions by these catalysts and $AlEt_3$ as a cocatalyst was carried out.

Ethylene polymerization

Polymerization of ethylene at similar condition for catalysts of S3 to S8 Table I and polymerization condition reported in Table II was carried out. Figure 4 shows the activity profiles of these catalysts.

TABLE II
Catalysts Polymerization Conditions

Catalyst				
Num	mg	$L_0 = P_{H2}/P_{C2}$	$L_1 = P_{H2}/P_{C2}$	$L_2 = P_{H2}/P_{C2}$
S3	30	0	0.29	0.67
S4	32	0	0.5	0.85
S5	33	0	0.4	1.25
S6	31	0	0.67	1
S7	30	0	0.75	1.6
S8	32	0	0.6	0.98

Polymerization condition: Al/Ti = 10 mol ratio, P_E = 6 bar, T = 85°C, Mixing = 600 rpm.

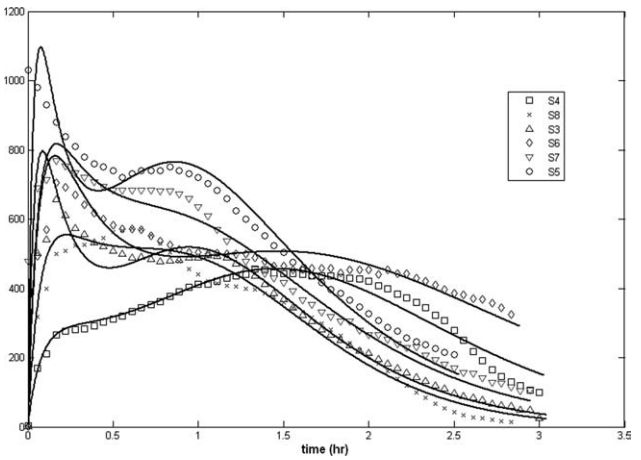

Figure 4 Rate-time profiles correspond to catalysts of Table I.

By considering and comparing these profiles, obviously, two or three distinguishable periods in each profiles can be observed.

Profile of catalyst S4 shows the lowest activity and gradually increasing activity trend. Given this profile, there are two identifiable stages, which in first stage, catalyst activity reaches initial maximum value in a short time, $\sim$ 20 min, and then take a short steady state and after that again gradually and linearly increases, and finally a decay trend starts appearing as a conventional catalyst. In the case of catalyst S3, a two stages period observed too, but with a discrepancy in first step which has a more increasing accelerating activity and reaches a higher initial activity than catalyst S4, second stage in contrast to its corresponding S4 stage shows a diminishing behavior.

For other catalysts, S5 to S8, parallel trends in activity profiles can be observed, but with higher activity in comparison with S3 and S4.

In general, it can be concluded that, catalyst with similar surface area, by increasing pore volume or pore size diameters, catalyst activity increases and the shape of rate-time profiles changes noticeably.

Approximately, for catalysts with pore value bigger than 1 mL/g and 100 Å pore diameters, the trend of activity profile tends to be similar, but higher pore volume give higher activity especially in early stages of polymerization.

Conclusively,we can say that;

1. First stages of activity profiles have similar trend but by increasing pore volume, higher activity were achieved.
2. In second stage of polymerization, by increasing pore volume, the upward trend from low value of activity altered to downward trend from high value.
3. Activity behavior after 1.5 h of polymerization tends to make the same rends for all catalysts which it means, they are independent of support specifications.

Hydrogen responsibility

Hydrogen is commonly used as a chain transfer agent to adjust the MW, and thereby, the processability of polymers. To investigate the effect of H_2 on performance of S3 to S8 catalysts of Table I, polymerizations of ethylene with two different levels of H_2 concentration were carried out. In Figure 5, the effect of H_2 on activity profiles have been illustrated. Here, the investigation was carried out to find out the relationship between catalyst support structure and H_2 responsibility with the aim of reducing the lessening activity effect of hydrogen and to increase catalyst H_2 responsibility. It was already mentioned that catalyst based on $SiO_2/MgCl_2$ shows higher responsibility and less decreasing effect on activity. The reason why SiO_2 based Ziegler-Natta catalysts have such an effect, it is not obvious. Here, we try to analyze the structure parameters in SiO_2 which affect on H_2 responsibility. It requires determination of catalyst H_2 responsibility as a quantitative value.

Keii et al.[33] used following relations, eq. (2) for low H_2 concentration and eq. (3) for high H_2 concentration, for fitting R_p data which present the effect of H_2 concentration on reduction of R_p

$$R_p = \frac{R_0}{1 + 0.082[\mathrm{H_2}]^{0.5}} \tag{2}$$

$$R_p = R_0 - 44.3[\mathrm{H_2}]^{0.5} \tag{3}$$

where R_0 is the rate of polymerization in the absence of hydrogen.

Wanke and coworkers[34] used linear combination of above relations for fitting R_p dependence on $[H_2]$ as shown in eq. (4).

$$R_p = R_0\left\{(1 - k_1[\mathrm{H_2}]^{0.5}) + \left(\frac{1}{1 + k_2[H_2]^{0.5}}\right)\right\} \tag{4}$$

R_p data of our work show a more complex trend as it was illustrated in Figures 4 and 5.

As, it was shown in Figure 4, differences in supports properties made differences in polymerization behaviors. Here, with the aim of quantitative comparing of these results, efforts was made to fit R_p data with conventional kinetics relations and therefore to derive the kinetic parameters. As it can be seen from Figures 4 and 5, because of presence of diffusion limitations and fragmentation phenomena

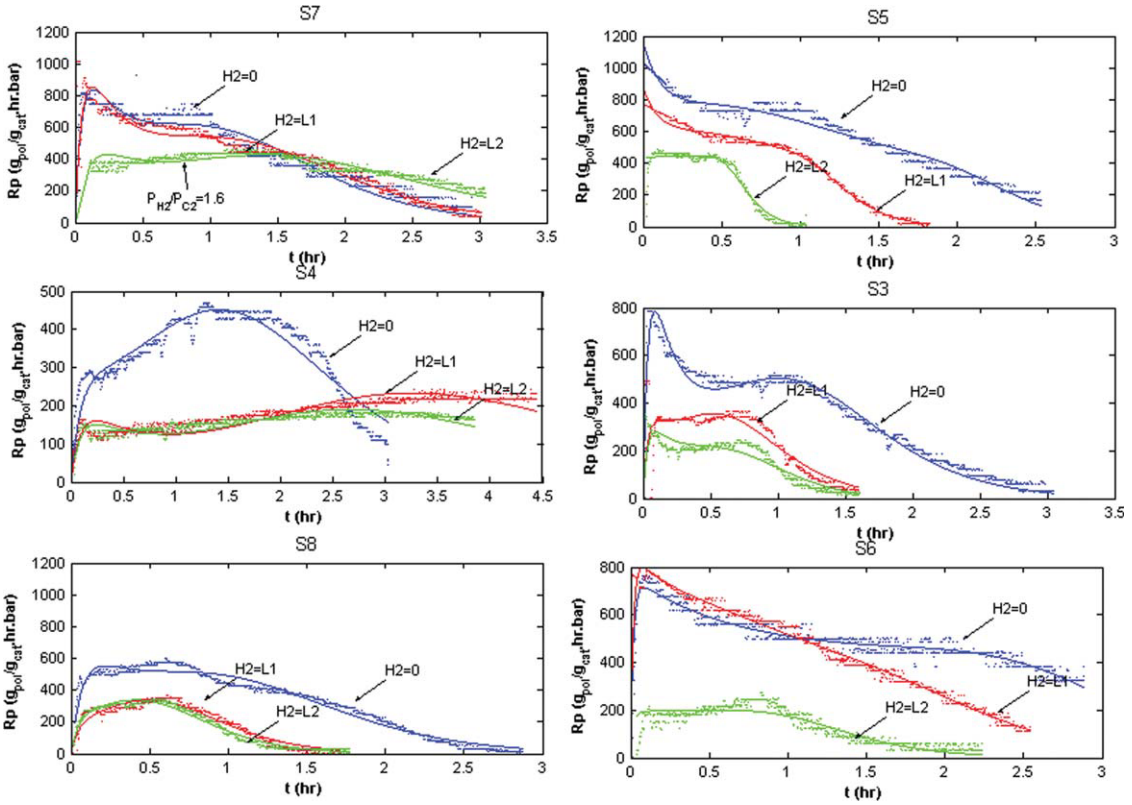

Figure 5 The effect of PH2/PC2 ratio on activity profiles of studied catalyst. [Color figure can be viewed in the online issue, which is available at www.interscience.wiley.com.]

in the growing particle during polymerization, the activity profiles gave more complex nature and it was impossible to fit R_p data with conventional presented equations. The main reason of these behaviors is the variety in support structure properties, which leads catalysts behavior altered during polymerization time due to the different fragmentation mechanisms.

Almost all researcher believe that fragmentations phenomena is essential for maintaining a sufficiently fast access of the monomer to active catalyst sites originally located within the pores of the support that affects the activity profiles and as mentioned before, has widely been studied in literatures and different models were proposed. A lot of investigations propose shrinkage model, also known layer-by-layer model. With respect to these experimental profiles, it was easy to bring to a close shrinkage model. Shrinkage fragmentation which depends on support physico-mechanical properties follows certain patterns. The major effect of fragmentation on activity profiles is the potential centers of catalyst which become available as function of time. Kinetic parameters of following relation which are derived on the base of conventional Ziegler-Natta mechanism, initiation, propagation and termination modeled by Kissin[35–37] are considered as a function of time.

$$\begin{aligned} R_P &= R \times [\exp(-k_d.t) - \exp(-k_a.t)] \\ R &= R_o \times \exp(-t/t_R) \\ K_d &= k_{do} \times \exp(-t/_{td}) \\ K_a &= k_{ao} \times \exp(-t/_{ta}) \end{aligned} \quad (5)$$

where R_p is experimental rate of monomer consumption at constant pressure, R, k_d, and K_a relates to average productivity, deactivation, and activation time functions, respectively.

To study, the effect of H_2 concentration on kinetic parameters and product properties, polymerization of ethylene was carried out in two levels of H_2 (P_{H2}/P_{C2}), L_1 and L_2, as reported in Table III with catalysts of Table I. The R_p data of Figure 4 were fitted by eq. (5) using CfTool subprogram MATLAB software and parameters of eq. (5) were derived and listed in Table III and as shown in Figure 6.

In Figure 6, the variations in R, K_d, K_a as a function of polymerization time are illustrated.

As, it is demonstrated in Figure 6 (column 1, $L_0 = P_{H2}/P_{C2} = 0$), for catalyst S4, R has a maximum value at whole time of polymerization, and other catalysts to be found in next steps according to increase in their pore volume diameter.

TABLE III
Kinetic Parameters of Studied Catalyst by Fitting Activity Profile According to Equation 5

Constant	S7	S5	S4	S3	S8	S6
R_1	4.17E+03	4.23E+03	5.73E+03	5.81E+03	6.06E+03	4.49E+03
R_2	5.92E+03	3.86E+03	1.89E+03	3.19E+03	4.29E+03	5.89E+03
R_3	2.76E+03	1.96E+03	1.98E+03	2.98E+03	3.26E+03	857.0833
td_1	0.3989	0.2956	0.5623	0.3388	0.42	0.6031
td_2	0.5329	0.2844	0.9176	0.2427	0.2402	0.5215
td_3	0.5428	0.1534	0.8637	0.2816	0.2208	0.2695
ta_1	1.0286	0.9085	0.6143	0.9136	0.7272	1.2356
ta_2	0.5509	0.308	2.0781	0.2621	0.2765	0.5258
ta_3	0.5708	0.1603	1.6296	0.2726	0.2349	0.3313
tr_1	0.7652	0.766	3.7044	0.6096	0.6642	1.1513
tr_2	1.7173	1.0131	2.1743	1.4476	1.425	1.8881
tr_3	0.5708	0.1603	1.6296	0.2726	0.2349	0.3313
kd_0	7.552	12.5234	6.2874	14.867	8.9844	6.8627
ka_0	11.607	23.56	7.0156	19.7535	10.4512	10.4403

Figure 6 shows bigger k_d for catalyst with lower pore volume diameter (PVD) that means, in same condition of polymerization, this catalyst have longer life time. Lower R_p and equal productivity can also be seen.

With regarding to Figure 6, it was observed that k_a for catalyst with higher pore volume is bigger than k_a of catalysts with lower pore volume especially for initial 15 min of polymerization, and generally, the presence of H_2 decreases k_a. On the other hand, the activation time of catalyst ($t = t_a$) is increased.

It was noticed that $R = \exp(-t/t_R)$ shows average productivity of catalysts.

Attention to these catalyst profile, it was concluded that by increasing average pore size diameters, the shape of profiles start changing from build-up to decay form, and with regard to this fact particle growth and fragmentation mechanism are

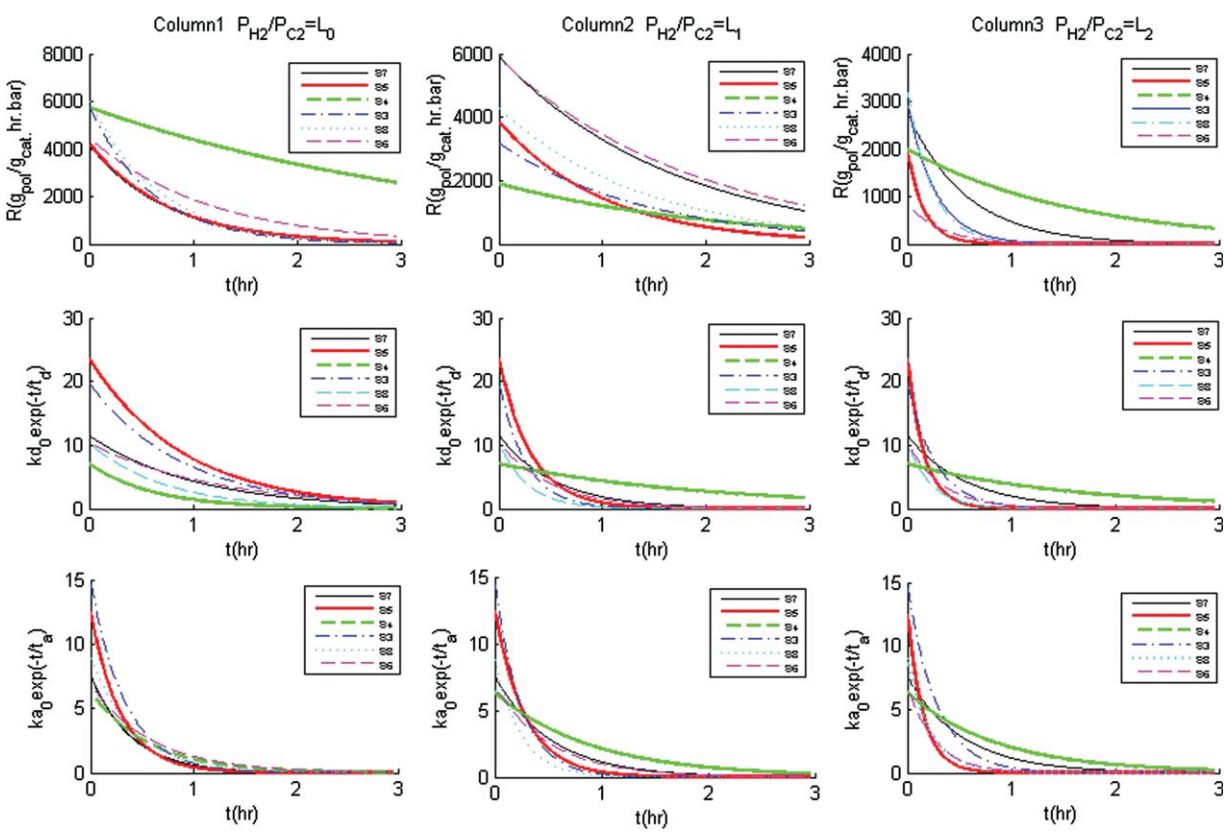

Figure 6 The comparison of the effects of PH2/PC2 on kinetic parameters. [Color figure can be viewed in the online issue, which is available at www.interscience.wiley.com.]

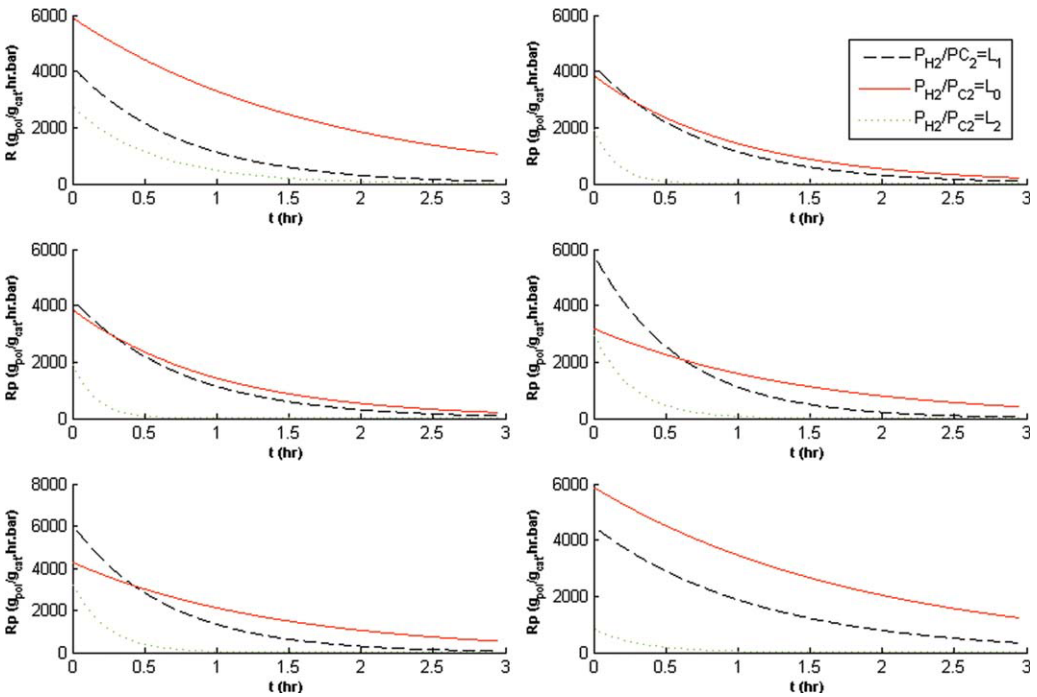

Figure 7 The comparison of [H2] effects on *R* in different catalysts. [Color figure can be viewed in the online issue, which is available at www.interscience.wiley.com.]

responsible for the profile activity shape, it can be proposed that progressive fragmentation occurs because of mechanical stresses which is created by polymer production for catalysts with small pore size (60 Å) and it can be described by layer-by-layer model fragmentation as suggested earlier.[7] In the case of a high pore volume catalyst, the monomer transports into the pores of the catalyst are more easier, and the polymer grows throughout the whole particle. The result is an immediate fragmentation of the catalyst particle known as the multigrain mode.[8]

For polymerizations which carried out in H_2 level 1 (column 2, $P_{H2}/P_{C2} = L_1$), in Figure 7, it was observed that *R* for S4 catalyst in comparison with the state without H_2 (column 1), considerably display a low value. While for other catalysts, with higher pore volume, *R* confirms no main reduction effect and even in some cases gives higher value. For polymerizations performed in the presence of much higher H_2 concentration, level 2, (column 3), it gave no further lowering effect on S4 catalyst, but for others considerable reducing effect was observed in assessment with Columns 1 and 2. As a conclusion of above discussions, we can say that, there are complex relationships between physico-chemical properties of supports (porosity, pore volume diameter, AQI,), polymerization conditions and activity profile of polymerization, and also strong interactions can be proved. For example, with increasing P_{H2}/P_{C2} ratio approximately to Level 1(column 2), the rate of polymerization for catalysts with high pore volume (pore volume diameter equal to about 200 Å) attest that the hydrogen give positive effect, although without H_2, catalysts with pore volume diameter <100 Å performs better performance.

In Table IV, changes in MFI and MFR of produced polymers with variation in P_{H2}/P_{C2} are illustrated. It is believed that MFI and MFR are indications of MW, and molecular weight distribution as major determinants of polymer properties. The results showed that for high pore volume catalysts, the responsibility of catalysts in increasing MFI are superior in contrast with catalysts with lower pore

TABLE IV
MFI Variation by Changing PH2/PC2 Ratio

Catalyst	(P_{H2}/P_{C2})[a]	MFI (g/10 min) (2.16 kg)	MFI (g/10 min) (5 kg)	MFR (5/2.19)
S3	$L_1 = 0.29$	1.2	4.9	4
	$L_2 = 0.67$	11	33.7	3
S4	$L_1 = 0.5$	1.4	4.1	2.9
	$L_2 = 0.86$	3.1	9.6	3
S5	$L_1 = 0.4$	4.2	11.3	2.7
	$L_2 = 1.25$	27.9	81	2.9
S6	$L_1 = 0.67$	1.3	4	3
	$L_2 = 1$	7.7	22.5	2.9
S7	$L_1 = 0.75$	2.2	7	3.2
	$L_2 = 1.6$	18.9	56.9	3
S8	$L_1 = 0.6$	7	21.5	3
	$L_2 = 0.98$	29.1	84.6	2.9

[a] For all catalysts, $L_0 = P_{H2}/P_{C2} = 0$ MFIs in similar condition were not measurable.

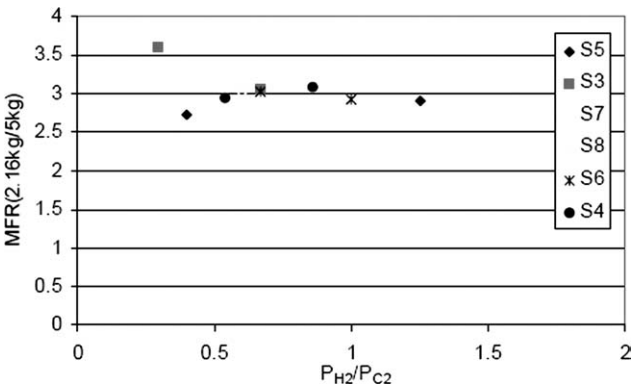

Figure 8 MFRs of catalysts of Table II with variation in PH2/PC2.

volume. Also in the same polymerization conditions, by increasing in pore volume diameter (PVD) of catalyst support the higher MFI can be obtained. Investigation of the MFR with variation in support specification and hydrogen concentration show interestingly no major change in their value, as shown in Figure 8.

CONCLUSIONS

A series of catalyst different in support specification was prepared and it was subjected to polymerization of ethylene.

The difference in structures of the used support showed a large influence on activity profiles and H_2 responsibility which suggests that the support characteristic change particle growth and mechanism of fragmentation during polymerization. It seems that among different factors, the pore size diameter of support have main effect on activity as well as kinetics profile and H_2 responsibility. It can be concluded that increasing pore diameters change fragmentation pattern from shrinking core to bisection mode and also give higher MFI and no major effect on MFR.

References

1. Ittel, S. D.; Johnson, L. K. Chem Rev 2000, 100, 1169.
2. Chadwick, J. C. Polym Sci Technol 2003, 6, 517.
3. Auriemma, F.; De Rosa, C. J Appl Cryst 2008, 41, 68.
4. Jorgensen, R. J.; Goeke, G. L.; Karol, F. J. U.S. Pat. 4,349,648 (1982).
5. Pater, J. T. M.; Weickert, G.; Loos, J.; Swaaij, W. P. M. Chem Eng Sci 2001, 56, 4107.
6. Andoni, A.; Chadwick, J. C.; Niemantsverdriet, H. J. W.; Thüne, P. C. J Catal 2008, 257, 81.
7. Kosek, J.; Stepanek, F.; Marek, M. Elsevier Amsterdam 2005, 30, 137.
8. Webb, S. W.; Conner, W. C.; Laurence, R. L. Macromolecules 1989, 22, 2885.
9. Grof, Z.; Kose, J.; Marek, M. Ind Eng Chem Res 2005, 44, 2389.
10. Hammawa, H.; Wanke, S. E. Polym Int 2006, 55, 426.
11. Grieken, R.; Carrero, A.; Suarez, I.; Paredes, B. Macromol Symp 2007, 259, 243.
12. Zheng, X.; Loos, J. Macromol Symp 2006, 236, 249.
13. Abboud, M.; Denifl, P.; Reichert, K. H. Macromol Mater Eng 2005, 290, 558.
14. Zheng, X.; Pimplapure, M. S.; Weickert, G. J. Macromol Rapid Commun 2006, 27, 15.
15. McDaniel, M. P. J Polym Sci Part A: Polym Chem Ed 1981, 19, 1967.
16. McDaniel, M. P. J Catal 2009, 261, 34.
17. Fink, G.; Steinmetz, B.; Zechlin, J.; Przybyla, C.; Tesche, B. Chem Rev 2000, 100, 1377.
18. Fink, G.; Tesche, B.; Korber, F.; Knoke, S. Macromol Symp 2001, 173, 77.
19. Pakkanena, T. T.; Ronkkoa, H. L.; Knuuttila, H.; Denifl, P.; Tuula, T. L. J Mol Catal A 2007, 278, 127.
20. Rnkka, H. L.; Korpelaa, T.; Knuuttilaa, H.; Pakkanena, T. T.; Deniflb, P.; Leinonenb, T.; Kemellc, M.; Leskel, M. J Mol Catal A 2009, 309, 40.
21. Ferrero, M. A.; Chiovetta, M. G. Polym Eng Sci 1987, 27, 1436.
22. Paredes, B.; Soares, B. P.; Grieken, R.; Carrero, A.; Suarez, I. Macromol Symp 2007, 257, 103.
23. Bartke, M.; Severn, J. R.; Chadwick, J. C. Tailor-Made Polymers Via Immobilization of Alpha-Olefin Polymerization Catalyst, Wiley–VCH Verlag GmbH & Co. KGaA: Weinheim, 2008.
24. Noristi, L.; Marchetti, E.; Baruzzi, G.; Sgarzi, P. J Polym Sci Part A: Polym Chem 1994, 32, 3047.
25. Horckov, B.; Grof, Z.; Kosek, J. Chem Eng Sci 2007, 62, 5264.
26. Conner, W. C.; Webb, S. W.; Spenne, P.; Jones, K. W. Macromolecules 1990, 23, 4742.
27. Hammawa, H.; Wanke, S. E. J Appl Polym Sci 2007, 104, 514.
28. Knoke, S.; Korber, F.; Fink, G.; Tesche, B. Macromol Chem Phys 2003, 204, 607.
29. Liu, B.; Fukuda, K.; Nakatani, H.; Nishiyama, I.; Yamahiro, M.; Terano, M. J Mol Catal A 2004, 219, 363.
30. Korach, Ł.; Czaja, K.; Kovaleva, N. Y. Europ Polym J 2008, 44, 889.
31. Hyde, j. R. Grace W R & Co. CA Pat. 811107 (1969).
32. Apecetche, M. A. Univation Technologies LLC. U.S. Pat. 7,259,125 (2007).
33. Keii, T. Stud Surf Sci catal 1986, 25, 1.
34. Huang, J. C. K.; Lacombe, Y.; Lynch, D. T.; Wanke, S. E. Ind Eng Chem Res 1997, 36, 1136.
35. Zheng, X.; Pimplapure, M. S.; Weickert, G.; Loos, J. e-Polymers 2006, 028, 1.
36. Kissin, Y. V.; Mink, R. I.; Nowlin, T. E.; Brandolini, A. J. J Polym Sci Part A: Polym Chem 1999, 37, 4281.
37. Kissin, Y. V. J Polym Sci Part A: Polym Chem 2001, 39, 1681.